1

The Climate System

In this chapter we will introduce the concept of the climate system. Section 1.1 starts by discussing the different components of this system and their interactions. Next, in Section 1.2., the forcing of the climate system is presented. Climate models form the main topic of Section 1.3 and, using results from a simulation of a state-of-the-art climate model, the mean atmospheric and oceanic general circulation is described in Section 1.4.

1.1 System Components

Although individual scientists' views on the climate system probably greatly differ, anyone would admit that it is a system displaying complicated spatial-temporal variability in many of its subsystems, such as the atmosphere, the oceans, the cryosphere, and the biosphere.

In a report to the NASA Advisory Council, Bretherton (1988) presented a sketch of the Earth system components and their interactions. The original figure (Bretherton, 1988) is often referred to as the *horrendogram* of the climate system. The simplification shown in Fig. 1.1 is useful for recognizing many of the subcomponents of the climate system and identifying their connections. The figure also provides a basis for understanding the transfer of properties (such as energy and mass) that are exchanged between these different subsystems. Examples of such interactions and associated fluxes are usually referred to as the energy cycle, the hydrological cycle, and several biogeochemical cycles (for example, the carbon, sulfur, and nitrogen cycles).

Multi-scale interactions between processes within and between the different components create the complicated behavior of observables (such as temperature) in the climate system. Large-scale motions induce smaller-scale ones through

The Climate System
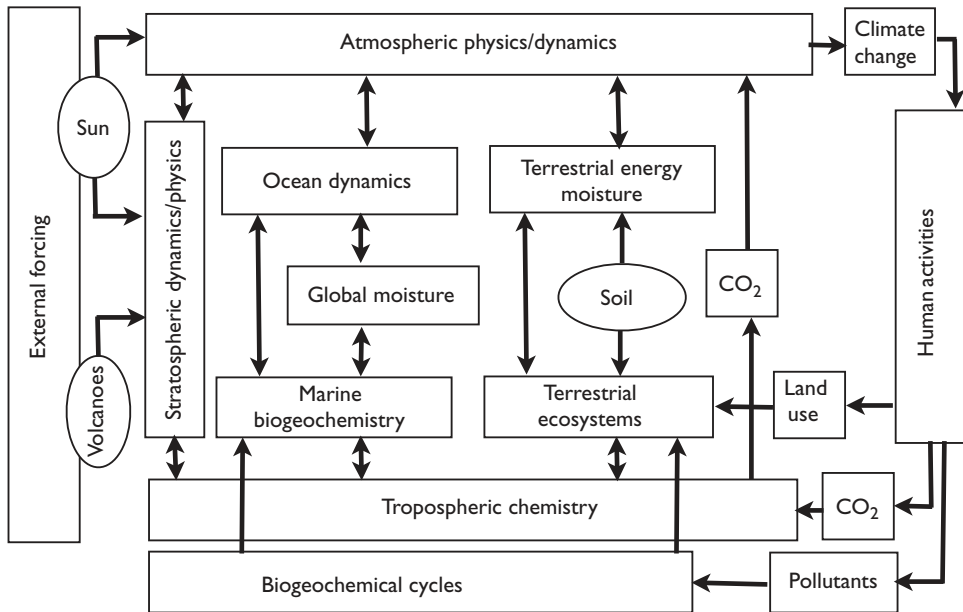
Figure 1.1 A schematic of the climate system showing the different components
and their connections (simplified from Bretherton, 1988). The arrows provide an
impression of the interactions between the components (one-way or two-way).

instabilities in a hierarchical cascade. In turn, the collective interaction of the
small-scale processes affects the development of the large-scale motions.

Cloud formation is one of those processes in which these features are clearly evi-
dent. A cloud is formed through the aggregation of water, by means of atmospheric
aerosol particles that act as initiation centers. The dimensions of these particles are
usually smaller than those of a typical grain of dust. The type and extent of the
resulting clouds will depend on the nature, concentration, and distribution of such
agents, together with the thermodynamical state of the external environment. This
mesoscopic characteristic will then impact, for example through rain, the longwave
absorption and shortwave reflection of radiation, and subsequently affect the large-
scale atmospheric motions.

Many feedback processes exist within and between the various components of
the climate system. An example is sea-ice albedo feedback, in which a reduction
in sea-ice extent will lead to less reflection of shortwave radiation and hence to a
further reduction in the sea-ice extent. The complex feedback web that is created in
this way, together with the forcing of the climate system (Section 1.2) gives rise to

complicated climate variability and makes the understanding of phenomena in the climate system and their prediction of future development a difficult task.

1.2 Forcing

There are several external forcing mechanisms of the climate system, the most important being the radiation from the Sun. Insolation is the amount of energy received by the Earth's surface in the form of shortwave radiation. The energy difference between the incoming solar radiation and the outgoing longwave radiation at the top of the atmosphere is the main source of energy in the climate system.

The Earth can be seen as a closed system to which heat is added, so that the first law of thermodynamics applies, i.e.,

$$dQ = dE - dW, \tag{1.1}$$

where dQ is the amount of heat added, dE is the change in internal energy of the system, and dW is the work extracted from the climate system (Hartmann, 1994). Since the work done by the Earth on its environment is negligible and the incoming energy from the Sun and the outgoing energy from the Earth are mainly radiative, the dominant energy balance of the Earth is a radiative balance. If the Earth is in thermodynamic equilibrium (i.e., its internal energy is constant), the radiative flux received by the Earth from the Sun must be balanced by the outgoing radiation emitted by the Earth.

The solar radiation flux incident upon the Earth at the top of the atmosphere, often referred to as the solar constant S, has a mean value of 1370 Wm^{-2}. It is a function of the luminosity of the Sun and is inversely proportional to the square of the Sun to Earth distance (James, 1994). However, the solar constant is not the flux received by the surface of the Earth. Indeed, the Earth's area normal to the Sun's beam is πr_0^2 while its total surface is $4\pi r_0^2$, where r_0 is the radius of the Earth. Furthermore, a fraction α of the incoming solar radiation is directly reflected to space. The quantity α is called the planetary albedo and has an average value of about 0.3; the local albedo varies strongly locally due to the presence of clouds, snow, and ocean water. Thus, a total incoming flux of

$$R_{in} = \frac{(1-\alpha)S}{4} \tag{1.2}$$

is received by the Earth's surface and must be balanced by outgoing radiation for the Earth to be in equilibrium.

The Stefan–Boltzmann law states that the radiation emitted by a black body in thermodynamic equilibrium (R_{out}) is uniquely related to its surface temperature T through

$\dfrac{S}{4} \downarrow$ $\uparrow \; \alpha \dfrac{S}{4}$ $(1-\epsilon)\sigma_b T_s^4 \uparrow$ $\uparrow$ $\sigma_b T_a^4$

Tₐ   **One-layer atmosphere**

$(1-\alpha)\dfrac{S}{4} \downarrow$ $\sigma_b T_s^4 \uparrow$ $\downarrow \; \sigma_b T_a^4$

Tₛ   **Surface layer**
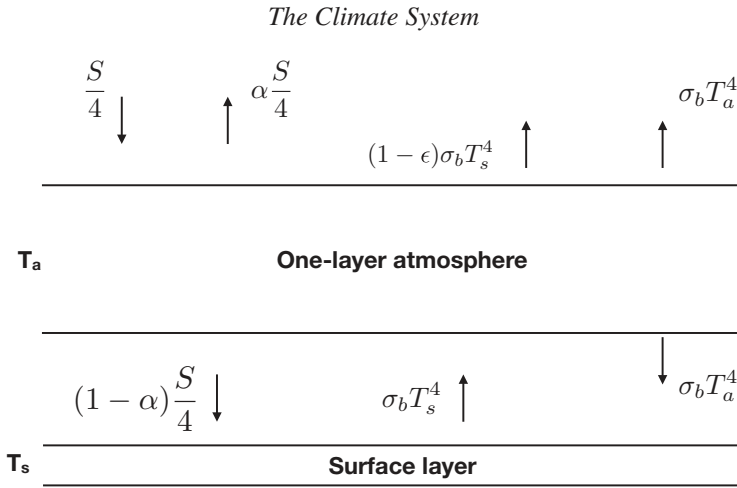
Figure 1.2 Sketch of an idealized model of the atmosphere to illustrate the greenhouse effect (after James, 1994).

$$R_{out} = \sigma_b T^4 , \tag{1.3}$$

where $\sigma_b = 5.67 \times 10^{-8}$ Wm^{-2} K^{-4} is the Stefan–Boltzmann constant. From the balance $R_{in} = R_{out}$, the equilibrium surface temperature T_e of the Earth is found from (1.2) and (1.3) as

$$T_e = \left(\frac{(1-\alpha)S}{4\sigma_b} \right)^{\frac{1}{4}} , \tag{1.4}$$

giving a value of $T_e = 255$ K for the Earth substituting the values for α, σ_b, and S given above (Hartmann, 1994).

The observed average temperature at the surface of the Earth is close to 288 K, which is considerably warmer than T_e. This temperature difference is explained by the Earth's atmosphere being relatively transparent to the incoming solar radiation but acting as a black body for outgoing terrestrial radiation (Hartmann, 1994). This mechanism is called the "greenhouse effect" and can be illustrated with a simple slab model of the atmosphere (Fig. 1.2).

The atmosphere is assumed completely transparent to incoming solar radiation R_{in} but to absorb a fraction ϵ of the infrared radiation R_{out} emitted by the Earth's surface (Fig. 1.2) and emit this in all directions. The radiative balance at the surface thus gives

$$R_{in} = R_{out} - R_a, \tag{1.5}$$

with $R_{out} = \sigma_b T_s^4$ and $R_a = \sigma_b T_a^4$ where T_s and T_a are the temperatures of the surface and of the atmosphere, respectively. Similarly, the radiative balance in the atmospheric layer is

$$\epsilon R_{out} = 2R_a. \tag{1.6}$$

From (1.4)–(1.6), we find

$$T_s = \left(\frac{2}{2 - \epsilon} \right)^{\frac{1}{4}} T_e, \tag{1.7a}$$

$$T_a = \left(\frac{\epsilon}{2 - \epsilon} \right)^{\frac{1}{4}} T_e. \tag{1.7b}$$

We can see that for an atmosphere totally opaque to infrared radiation, $\epsilon \to 1$, the temperature of the atmosphere T_a is the emission temperature T_e and the surface temperature is warmer than the overlying atmosphere. For a typical value of $\epsilon = 0.771$, the temperature $T_s = 288$ K, close to what is observed, while the temperature of the atmosphere is colder, $T_a = 227$ K. It is worthwhile noting that the value of ϵ is controlled by the concentrations of greenhouse gases in the atmosphere which absorb radiation in the infrared band. The main contributors are carbon dioxide, methane, and water vapor, providing about 80% of the current greenhouse effect (Hartmann, 1994).

Radiative balance models explain to first order the global annual mean temperature of the Earth. However, the incoming solar radiation is not uniformly distributed over the planet as it is large in the tropics and small in polar regions. At the same time, outgoing longwave radiation is relatively uniform with latitude. This leads to an energy imbalance in which the tropics are continuously gaining heat while the polar regions lose heat, hence creating a meridional temperature gradient. This gradient drives the atmospheric and oceanic circulations that redistribute energy on the planet and are important for understanding the observed climate variability.

1.3 Climate Models

Observations are crucial to the study of climate variability, but the records are very limited (see Chapter 3). As we also cannot investigate climate variability phenomena in the laboratory, climate models are a central tool in climate research. A wide range of models is in use, from conceptual climate models to state-of-the-art global climate models (GCMs). It would be impossible (and rather useless) to try to provide an overview of all the models that are being used at the moment in the climate research community.

Scales and processes are important properties of climate variability, and this motivates a classification of climate models using these two traits (Fig. 1.3). Here the trait "scales" refers to both spatial and temporal scales as there exists a relation between both: on smaller spatial scales, usually faster processes take place. "Processes" refer to either physical, chemical, or biological processes taking place in
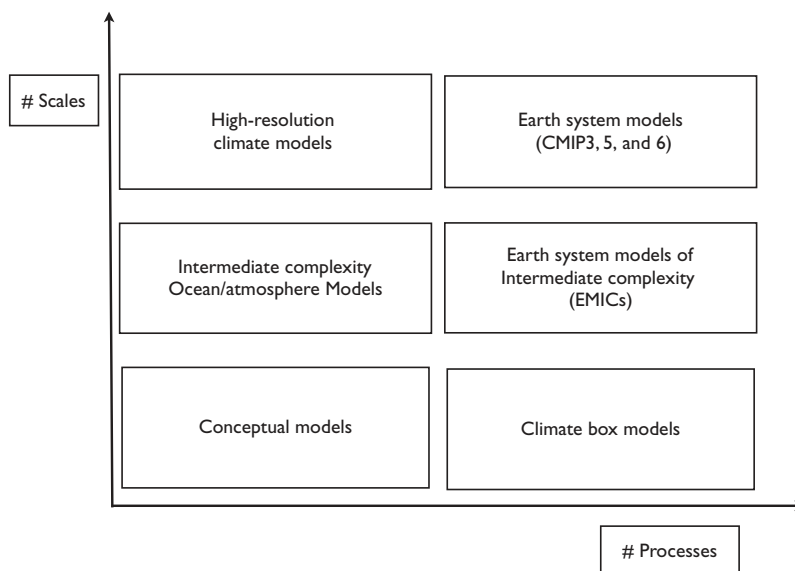
Figure 1.3 Classification of climate models according to the two model traits number of processes and number of scales. There is of course overlap between the different model types, but for simplicity they are sketched here as nonoverlapping.

the different climate subsystems (atmosphere, ocean, cryosphere, biosphere, lithosphere).

Models with a limited number of processes and scales are usually referred to as conceptual climate models. In these models only very specific interactions in the climate system are described. An example is the models of glacial–interglacial cycles (Saltzmann, 2001) formulated by small-dimensional systems of ordinary differential equations. For example, only the interactions of the ice sheet volume, atmospheric CO_2 concentration, and global mean ocean temperature are included.

Limiting the number of processes, scales can be added by discretizing the governing partial differential equations spatially up to three dimensions. A higher spatial resolution and inclusion of more processes will give models located in the right upper part of the diagram Fig. 1.3. In a GCM (Fig. 1.4), we divide the atmosphere, ocean, ice, and land components into grid boxes. Over such a grid box we consider the budgets of momentum, mass, and, for example, heat. The difference between what goes into a box minus what comes out of that box (e.g., heat) leads to an increase/decrease of a particular quantity (e.g., temperature). Once the distribution of a quantity is known at a certain time, then these budgets provide an evolution equation to determine the quantity some time later.
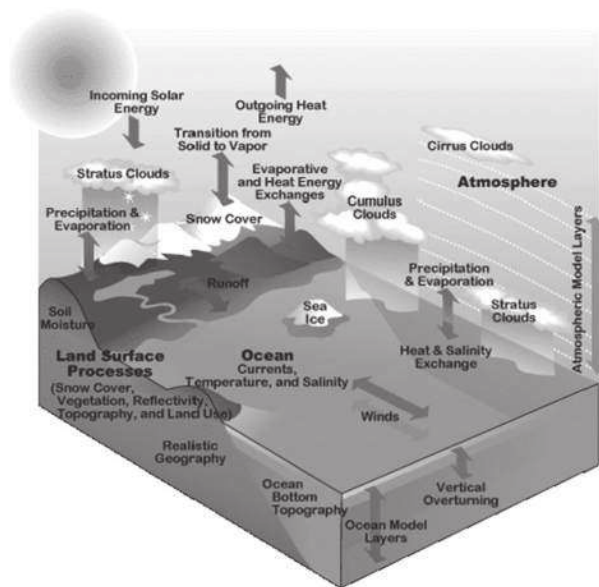
Figure 1.4 An overview of the components of the Community Earth System Model (CESM, see www.cesm.ucar.edu).

The advantage of more boxes is that we resolve the temperature more accurately (more points in a certain area). With an increasing number of grid boxes, however, the time evolution of an increasing number of quantities (at each grid box) has to be calculated. The same holds for the number of processes included in a GCM: more processes simply means more calculations. Also, the longer the time period over which we want to compute the evolution of each quantity, the longer it takes to do the calculation on a computer.

The state-of-the-art GCMs are located above the Earth System Models of Inter-mediate Complexity (EMICs; Claussen et al., 2002). Compared to GCMs, the ocean and atmosphere models in EMICs are strongly reduced in the number of scales. For example, the atmospheric model may consist of a quasi-geostrophic or shallow-water model and the ocean component may be a zonally averaged model. The advantage of EMICs is therefore that they are computationally less demanding than GCMs and hence many more long-timescale processes, such as land-ice and carbon cycle processes, can be included. Each of the individual component models of EMICs may also be used to study the interaction of a limited number of processes. Such models are usually referred to as *Intermediate Complexity Models* (ICMs). A prominent example is the Zebiak–Cane model of the El Niño/Southern Oscillation phenomenon (Zebiak and Cane, 1987). In time, the GCMs of today will be the

EMICs of the future and the state-of-the-art GCMs will shift toward the upper-right corner in Fig. 1.3.

In the remainder of this chapter, we describe the mean state of the climate system as determined from a high-resolution climate-model simulation. Although these mean fields deviate from observations in several aspects, the advantage of this approach is that the fields are dynamically consistent in that the basic conservation laws are satisfied.

1.4 Mean State

Model output from a recent about 250-year Community Earth System Model (CESM) simulation is used, where the ocean component (the Parallel Ocean Program, POP), as well as the sea-ice model have a $0.1°$ resolution (van Westen and Dijkstra, 2017). There are 42 (non-equidistant) vertical levels in the POP model, with highest resolution near the ocean surface. The atmosphere and land surface model have a horizontal resolution of $0.5°$, and 30 non-equidistant pressure levels are used in the atmosphere model. The forcing conditions (e.g., CO_2, solar, aerosols) are those observed over the year 2000 (repeated for every model year). The model output analyzed has a monthly resolution.

Two time series are shown in Fig. 1.5 to illustrate the equilibration of this simulation. The global mean surface temperature and radiative imbalance at the top of the atmosphere start equilibrating after about 150 years, with only a small positive value of the global mean radiative imbalance over the last 100 years of the simulation (Fig. 1.5). In the analysis of the CESM results that follow, we will take the mean over the model years 170–199 (also often referred to as the climatology).
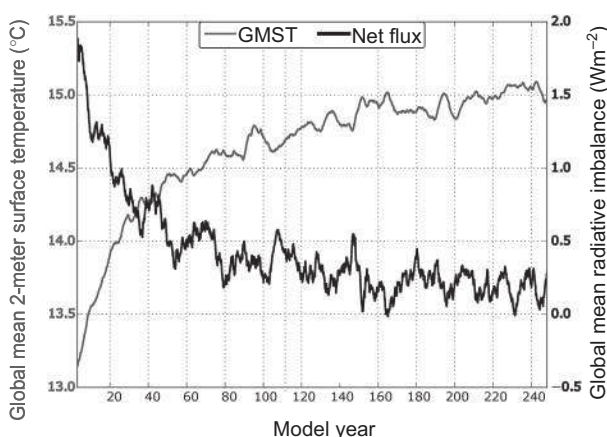

Figure 1.5 Equilibration of the CESM simulation, shown through the global mean surface (2 m) temperature and global radiative imbalance at the top of the atmosphere.
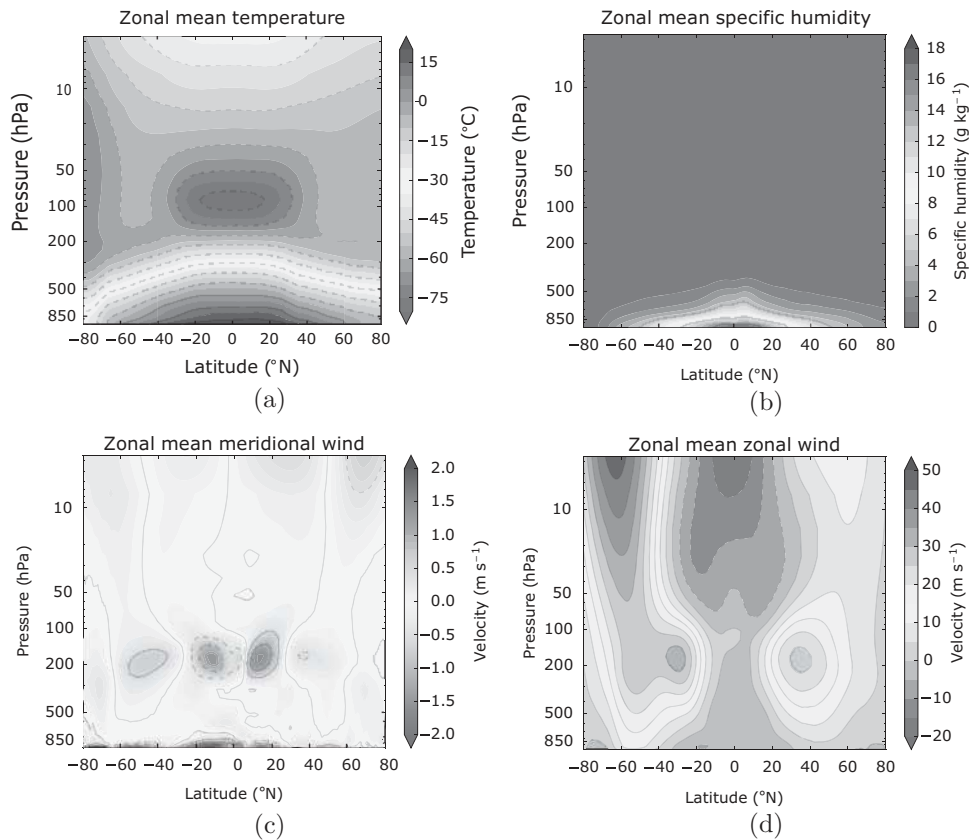
Figure 1.6 (a) Zonal mean temperature, (b) zonal mean moisture, (c) zonal mean meridional velocity, and (d) zonal mean zonal velocity. All fields are obtained by averaging over the CESM model years 170–199. (A black and white version of this figure appears in some formats. For the color version, please refer to the plate section.)

1.4.1 Atmosphere

The zonal mean temperature distribution (Fig. 1.6a) corresponds to that expected from the radiation balance, with relatively high surface temperatures in the tropics and low temperatures at the poles. As warm air can hold more moisture than cold air, also the specific humidity field (Fig. 1.6b) has a similar spatial structure as the temperature field, with high humidity in the tropics. The temperature decreases vertically up to a height of 100 hPa (according to mechanisms discussed in the previous section) but then increases again with height due to the presence of ozone.

Important characteristics of the mean circulation of the atmosphere can be analyzed from vertical-meridional cross-sections of the zonal mean zonal and meridional wind velocities (Fig. 1.6c, d). Over the latitudes 30°S–30°N, the dominant

feature is a clockwise cell in the Northern Hemisphere and an anti-clockwise cell in the Southern Hemisphere. There are surface equatorward winds and upper poleward winds, with air ascending at the equator and descending in the subtropics (Fig. 1.6c). This cell is referred to as the Hadley cell and is thermally direct, as a parcel of air following the cell will transport energy away from the equator. Thus, the Hadley circulation is forced by the meridional gradient of net radiative fluxes and converts the resulting available potential energy into kinetic energy. Another prominent feature is the strong westerly winds in the upper levels at the poleward limit of the Hadley cell, which is referred to as the subtropical jet. These jets are, to a good approximation, in thermal wind balance with the meridional temperature gradient (Fig. 1.6d).

The positions of the Hadley cell and the jet cores and intensity depend strongly on the season. As the insolation maximum moves poleward it is followed by the Hadley cell, while the jet intensity becomes stronger in the winter hemisphere. The extent of the Hadley cell is constrained by conservation of angular momentum and can be deduced by conceptual models (James, 1994). An extension further than the tropics would require very strong westerly winds in the upper levels, which would eventually become unstable, even in the presence of friction. Thus, poleward transport of heat north of the tropics must be taken over by another type of circulation.

A second circulation, the Ferrel cell, is visible poleward (Fig. 1.6c) of the Hadley cell. It is weaker and thermally indirect, implying that it is a sink of kinetic energy and must be forced by mechanical stirring. Indeed, strong eddy activity takes place in this region (Fig. 1.6d), where the eddies are able to transport air parcels poleward in the upper levels. The Ferrel cell is therefore able to transport heat poleward via the transient eddy heat fluxes, reducing the temperature gradient and wind shear generated by the Hadley circulation. The high-frequency transient eddies (periods of less than 10 days) are due to baroclinic instability and convert the available potential energy to eddy kinetic energy.

1.4.2 Ocean

On the large scale, the ocean circulation is driven by momentum fluxes (wind stress) and affected by fluxes of heat and freshwater at the ocean–atmosphere interface. The mean sea surface temperature field (Fig. 1.7a) shows that northern latitudes in the North Atlantic are much warmer than those in the Pacific, which is related to the pattern of the meridional overturning circulation (MOC), as discussed below. The MOC is also the reason that the surface salinity in the North Atlantic is about 2 g kg^{-1} greater than that in the North Pacific (Fig. 1.7b).